

Article

Observation of Ultra-Low-Frequency Wave Effects in Possible Association with the Fukushima Earthquake on 21 November 2016, and Lithosphere–Atmosphere–Ionosphere Coupling

Masashi Hayakawa ^{1,2,*}, Alexander Schekotov ³ , Hiroki Yamaguchi ^{4,†} and Yasuhide Hobara ^{5,6}

¹ Hayakawa Institute of Seismo Electromagnetics Co., Ltd. (Hi-SEM), UEC (The University of Electro-Communications) Alliance Center #521, 1-1-1 Kojima-cho, Chofu 182-0026, Japan

² Advanced & Wireless Communications Research Center (AWCC), The University of Electro-Communications (UEC), 1-5-1 Chofugaoka, Chofu 182-8585, Japan

³ The Schmidt Institute of Physics of the Earth, Russian Academy of Sciences, 10-1 Gruzinskaya, Moscow 123242, Russia; sasha.schekotov@gmail.com

⁴ Fuji DR Security Co., Ltd., 9 Iwato-cho, Shinjuku, Tokyo 162-0832, Japan; hiroki_01_yamaguchi@jp.honda

⁵ Department of Computer and Network Engineering, The University of Electro-Communications (UEC), 1-5-1 Chofugaoka, Chofu 182-8585, Japan; hobara@uec.ac.jp

⁶ Center for Space Sciences and Radio Engineering, The University of Electro-Communications (UEC), 1-5-1 Chofugaoka, Chofu 182-8585, Japan

* Correspondence: hayakawa@hi-seismo-em.jp; Tel.: +81-424-444-6349

† Current address: Quality Innovation Center Tochigi, Honda Motor Co., Ltd., Tochigi 321-3325, Japan.

Abstract: The study presents seismogenic ULF (ultra-low-frequency) wave effects, as observed at our own new magnetic observatory at Asahi (geographic coordinates: 35.770° N, 140.695° E) in Chiba Prefecture. Our target earthquake (EQ) is a huge one offshore of Fukushima prefecture (37.353° N, 141.603° E) with a magnitude (M) of 7.4, which occurred at 20.59 h on November 21 UT, 2016. As a sampling frequency of 1 Hz was chosen for our induction magnetometer, we could detect both ULF wave effects: ULF radiation from the lithosphere, and the ULF depression effect, indicative of lower ionospheric perturbations. Observing the results of polarization analyses, we detected clear enhancements in ULF (frequency = 0.01–0.03 Hz) lithospheric radiation 14 days, 5 days, and 1 day before the EQ, and also observed a very obvious phenomenon of ULF (0.01–0.03 Hz) depression just 1 day prior to the EQ, which is regarded as the signature of lower ionospheric perturbations. These findings suggest that pre-EQ seismic activity must be present in the lithosphere, and also that the lower ionosphere was very much perturbed by the precursory effects of the Fukushima EQ. These new observational effects from our station have been compared with our previous investigations on different seismogenic topics for the same EQ, including the ULF observations at another magnetic observatory at Kakioka, belonging to the Japan Meteorological Agency (JMA), about 50 km north of our Asahi station, subionospheric VLF/LF propagation data (Japanese and Russian data), AGW (Atmospheric gravity wave) activity in the stratosphere, and satellite observation of particle precipitations. We have found that seismogenic anomalies of different parameters tend to happen just around the EQ day, but mainly before the EQ, and have found the chain-like tendency of the effects of the lithosphere, which seem to propagate upwards the lower ionosphere. Finally, we will try to gain a better understanding of the physical phenomena or mechanisms of the lithosphere–atmosphere–ionosphere coupling (LAIC) process during the EQ preparation phase.

Keywords: earthquake (EQ) precursors; lithospheric ULF radiation; ULF depression effect; multi-parameter observation; lithosphere–atmosphere–ionosphere coupling (LAIC)



Citation: Hayakawa, M.; Schekotov, A.; Yamaguchi, H.; Hobara, Y. Observation of Ultra-Low-Frequency Wave Effects in Possible Association with the Fukushima Earthquake on 21 November 2016, and Lithosphere–Atmosphere–Ionosphere Coupling. *Atmosphere* **2023**, *14*, 1255. <https://doi.org/10.3390/atmos14081255>

Academic Editors: Xin-Yan Ouyang, Xuemin Zhang and Peng Han

Received: 26 June 2023

Revised: 31 July 2023

Accepted: 4 August 2023

Published: 7 August 2023



Copyright: © 2023 by the authors. Licensee MDPI, Basel, Switzerland. This article is an open access article distributed under the terms and conditions of the Creative Commons Attribution (CC BY) license (<https://creativecommons.org/licenses/by/4.0/>).

1. Introduction

Short-term earthquake (EQ) prediction is one of the most important subjects left in geosciences, and is of vital importance for human beings to mitigate natural disasters [1–6].

During the last few decades there have been extensive investigations on the precursory phenomena of EQs for short-term EQ prediction, and enormous progress has been made regarding various kinds of non-seismic, especially electromagnetic EQ precursors [7–9]. It has recently been agreed, based on a huge amount of subionospheric VLF/LF observation (e.g., [10–14]), ionosonde observation, satellite-based GPS (global positioning system) TEC (total electron content) observation (e.g., [15,16]), and in-situ satellite plasma and wave observations [17–23], that the ionosphere is extremely sensitive to pre-seismic lithospheric activity, and this has been suggested to be the most promising candidate for short-term EQ prediction, even though the mechanism through which the ionosphere is perturbed by the influence of lithospheric activity is still controversial [1–6]. So, the recent greatest concern of our seismo-electromagnetic studies is elucidation of the mechanism of lithosphere–atmosphere–ionosphere coupling (LAIC) [1–8]. In order to investigate the LAIC process, multi-parameter observation is highly recommended (e.g., [1–6]); this refers to the combined observation of various parameters of lithospheric, atmospheric and ionospheric perturbations, with the full use of ground- and satellite-based observational data (see, e.g., [24–28]). Alongside these seismo-ionospheric perturbations, Hayakawa et al. [29,30] have suggested further promising candidates for short-term EQ prediction, which are the electromagnetic wave phenomena in ULF/ELF (extremely low-frequency) bands, including (i) ULF direct radiation from the lithosphere, (ii) the ULF depression effect (as the signature of lower ionospheric perturbations), (iii) ULF/ELF radiation in the atmosphere, and (iv) anomalies in Schumann resonances. The first and second topics will be considered in this paper.

Since we have established our own magnetic field measurements at Asahi (geographic coordinates: 35.770° N, 140.695° E) in the Chiba prefecture, the purpose of this paper is to present some new evidence on the two ULF wave effects of (i) lithospheric direct ULF radiation, and (ii) ULF depression (as the depletion of ground-based horizontal magnetic fields), involved in a rather huge EQ ($M = 7.4$) offshore of Fukushima prefecture on 21 November UT, 2016, using the data from our observations at Asahi.

Initially, we comment on the observation of lithospheric ULF radiation. Many papers on ULF lithospheric radiation (e.g., [31–44]) have been published recently. However, it is highly invaluable to describe historical events within the ULF magnetic field variations before huge EQs, as typical examples. The unprecedented ULF signature was first reported at Kodiak 2 h before the great Alaska EQ (M (magnitude) = 7.2) of 27 March 1964 [45]. Local ULF signals with high amplitude were observed near the epicenters of violent M (magnitude (surface)) >7 EQs in Loma Prieta, California [46] and Spitak, Georgia [47,48]. Another was observed for the 1993 Guam EQ (3 August 1993, $M = 8.0$) [49]. The important findings from these large EQ events are summarized below [50–56].

- (1) The main frequency range of lithospheric direct radiation is located at ULF around $f = 0.01$ Hz (period = 100 s), probably because of the skin effect of wave propagation in the lithosphere.
- (2) Magnetic field intensity seems to exhibit an increase about one week (5–12 days) before an EQ, followed by a quiet period (quiescence), and an abrupt intensity increase just before (i.e., less than one day before) the EQ. The intensity ranges from a few nT to tens of nT.
- (3) The presence or absence (or detectability) of a ULF anomaly at a station is empirically expressed using the threshold of $0.025 R$ (epicentral distance (in km)) = $M - 4.5$ [29,50]; e.g., $R = 70$ km for $M = 6$, and $R = 100$ km for $M = 7$. The most peculiar feature of this ULF radiation is that ULF radiation observation itself is a typical “local” measurement; i.e., a ULF observatory can sense only the region close to the observatory (within 100 km or so).

Subsequently, we will review another ULF phenomenon in this paper, that is, the depression of ULF horizontal magnetic field components. The first report on the depression of ULF horizontal magnetic fields observed on the ground was produced by Molchanov et al. (2003, 2004) [57,58], and later confirmed on the basis of long-term observation [59] and some other case studies [60–64]. This effect is characterized by the depression (or depletion)

of the horizontal magnetic field component of ULF waves as observed on the ground, irregular pulsations (Pi's) mainly coming from the magnetosphere at night. These are in a frequency ($f \simeq 0.01$ Hz) [29] that is similar to that of lithospheric ULF emissions detected on the ground, which are likely due to the lower ionospheric perturbation [29,57,58]. The important features of this phenomenon are summarized as follows.

- (1) A few days before an EQ, we observe a decrease in ground-based horizontal magnetic field fluctuations of nighttime irregular pulsations in the vicinity of local midnight.
- (2) This is essentially noticeable within the ULF frequencies, especially in the frequency ranges of 0.03–0.05 Hz.
- (3) The absolute value of ULF depression is found to depend linearly on the local seismicity (or M), exhibiting a scaling law that is more pronounced for larger M EQs.
- (4) Despite of the same local measurement with ULF lithospheric radiation, the sensing range of the ULF depression effect is likely to be much larger than that of lithospheric radiation.

2. EQs Used in This Paper

A significant enhancement in seismic activity was observed, particularly on the Pacific Ocean side of Japan, probably in the form of aftershocks from the disastrous 2011 Tohoku EQ (in the seismological sense); our target EQ is considered to be one of those aftershocks. This EQ happened at 20 h 59 m on 21 November 2016 (UT); its magnitude via JMA was (M) = 7.4, with depth = 11 km, and its EQ epicenter is located at the geographic coordinates of (37.353° N, 141.603° E). This EQ happened inside the crust of the continental plate, with a normal fault type. Thus, we have studied a period of plus/minus 1 month around this main EQ. Figure 1 illustrates the map of our Asahi ULF station (ASA), and large EQs including our target EQ (21/11/16). The other EQs in the figure are the EQ that occurred on 23/11/16, which was just an aftershock of our target EQ, and another is the 11/11/16 EQ offshore of the Miyagi prefecture ($M = 5.8$, $d = 68$ km). The last one is an EQ in the western part of Japan, in Tottori, which occurred on 21/10/16 ($M = 6.6$, $d = 11$ km), and is located too far from our ULF station to have any influence on the ULF data at Asahi. In the following, we will discuss whether any observed anomalies are related to any one of these EQs.

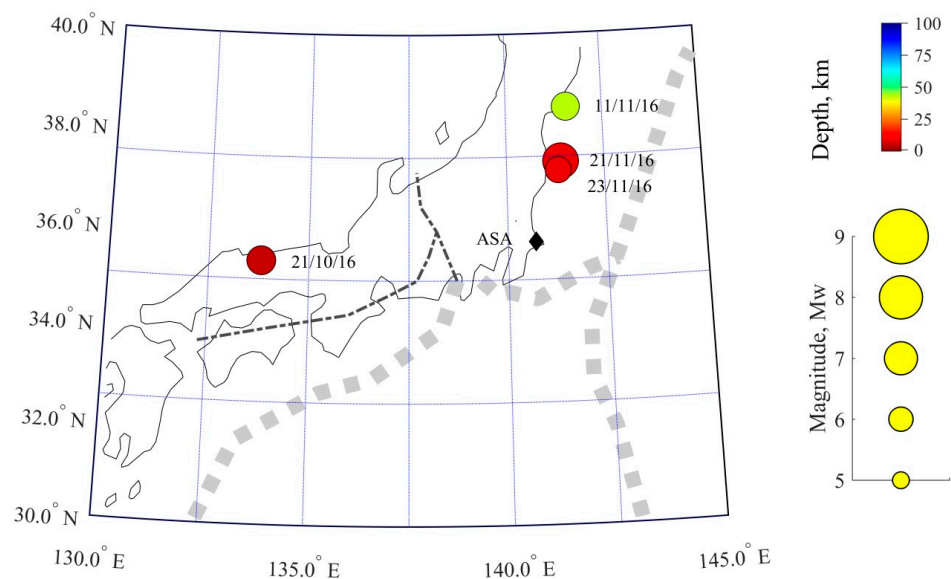


Figure 1. Locations of our new ULF observatory at Asahi (ASA) (black rhombus), and epicenters of the EQs (circles) during the period around the target EQ (21/11/16). The size of the circle indicates EQ magnitude, and its color refers to EQ depth. The wide gray dashed lines refer to the position of the trenches, and the thin black dash/dot lines on the mainland indicate the location of the main faults.

Here, the local seismicity at an observing station is studied using an index K_{LS} :

$$K_{LS} = \frac{10^{0.75M_L}}{10(R + 100)} \quad (1)$$

where R is the epicentral distance from the observation station to the EQ epicenter (in km), and M_L is the local EQ magnitude (but essentially the same as M in other places). This index was introduced by Molchanov and Hayakawa (2008) [8] to study seismo-acoustic emissions. With this index, they take into account the attenuation of seismic waves in the Earth's crust, even though low frequency waves propagate in the Earth-ionosphere waveguide with very small damping.

According to the formulas [65,66], the maximum size (or radius) of the EQ preparation zone is estimated to be about 1,500 km with this EQ M , so the observatory of ASA is well within the radius of this EQ preparation zone. Another more important quantity, called the critical zone for EQ preparation, is defined by Bowman et al. (1998) [67] based on the self-organized effect in the lithosphere, which is about 299 km for our EQ magnitude; therefore, our observatory at Asahi is within this critical zone. Thus, it is expected that we could find any significant seismogenic phenomena, due to the self-organization of the lithospheric fault zone.

Furthermore, it is very important to note whether any observed anomaly is related to any space weather perturbations (solar activity, geomagnetic activity, etc.); hence, we have already extensively studied the conventional geomagnetic activity index, Dst, and Kp index, taken from World Data Center at Kyoto, in our previous several papers [68–70]. It was concluded that the time period around this Fukushima EQ is rather geomagnetically quiet, and free from any conspicuous geomagnetic disturbances. Additionally, we found no significant meteorological disturbances during the period in this area.

3. ULF Observation and Analysis Methodology

3.1. ULF Data

We established our own ULF observatory at the beginning of 2016, and have since continued observation. This station is located at Asahi (ASA) (geographic coordinates: 35.770° N, 140.695° E) in the Chiba prefecture; this observatory is about 50 km south of the famous Kakioka Magnetic Observatory belonging to JMA (36.23° N, 140.18° E). While a fluxgate magnetometer is used at Kakioka, we use an induction-coil magnetometer LEMI 30 (produced by a Ukrainian Lviv group) with a data logger. Our complete system consists of three induction systems (horizontal x , y , and vertical z components), and the possible frequency range is from 0.001 Hz (1 mHz) to 30 Hz. However, when we started the observation at Asahi, we chose a sampling frequency of 1 Hz in order to pay more attention to ULF wave phenomena, and to avoid accumulating a huge amount of data when observing the higher frequency phenomena of ULF/ELF atmospheric radiation [64]. Recently, we have changed this sampling frequency to 128 Hz.

3.2. Methodology of ULF Data Analysis

3.2.1. Lithospheric ULF Radiation

With the use of ULF magnetic field data, we can initially investigate the well-known electromagnetic radiation from the lithosphere, as mentioned before (e.g., [50–55]), which has recently been extensively studied all over the globe, gaining a lot of attention [31–56].

After an extensive analysis of all-day ULF data for whole days, we found that daytime data are contaminated by artificial man-made noise, even though this station is situated in the suburbs of a small town (however, it is in the highly populated Tokyo district). Thus, we used only the nighttime data (only UT = 16–20 h or LT (JST) = 01–05 h, 4 h interval) for further analyses. Sometimes, when there existed some artificial noise at night, we replaced those missing data with an appropriate method in such a way that the response on all the panels in Figure 2 at that time would be minimal, or close to zero.

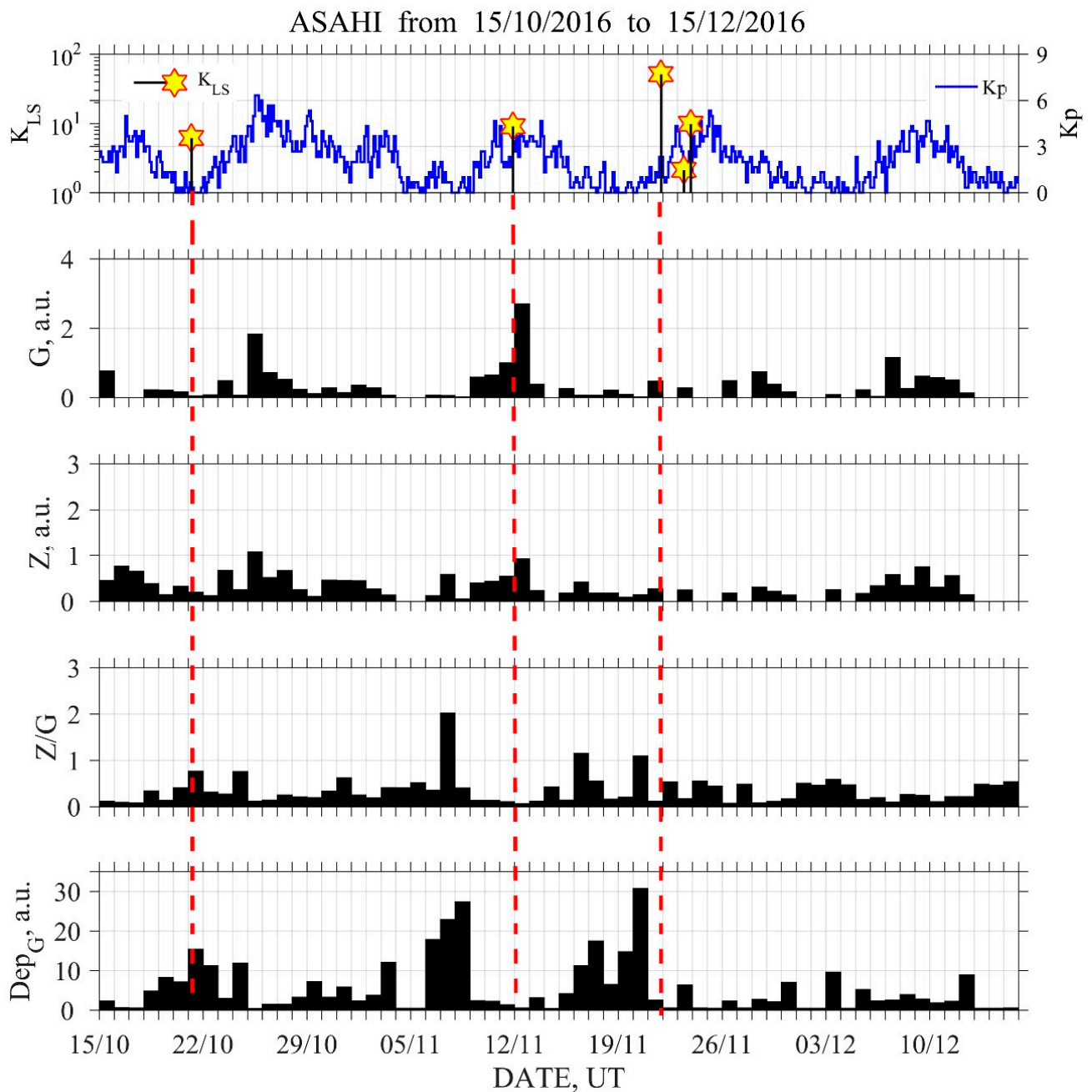


Figure 2. The evolutions of seismicity, geomagnetic activity, and ULF magnetic field characteristics in the two-month interval around the date of our EQ on 21 November, 2016. The top panel indicates the temporal evolutions of the local seismicity index K_{LS} (as yellow stars) and the geomagnetic activity Kp index (in blue). The average values of the horizontal G , vertical Z component and their ratio Z/G (or polarization) are presented on the next three panels. The evolution of depression Dep_h is depicted in the bottom panel. Vertical red broken lines refer to the occurrence times of the EQs of interest.

Using 1 s sampling ULF data at Asahi, we estimated the daily power spectral densities of the total horizontal magnetic field component, G , and the vertical component, Z , at different frequencies, as follows. The waveforms of three field components during each interval of 30 min were subjected to an FFT analysis, and the power spectral density data for one day at a particular frequency consist of eight intervals, because the night duration is 4 h. We then used their average as a daily value. Then, the polarization of Z/G was estimated every 30 min, and we took their average as the power ratio at each frequency,

which was initially proposed by Hayakawa et al. (1996) [49]; furthermore, Currie and Waters (2014) [56] confirmed the usefulness of this parameter in distinguishing seismogenic ULF radiation from other noises, including space pulsations. Most recent ULF works are based on analyses of this polarization parameter [35–38,40–42].

3.2.2. ULF Magnetic Field Depression

Even when using the same ULF data, we can study a new aspect of ULF wave phenomena: the depression of ground-based ULF horizontal magnetic field components. This effect was initially discovered by Molchanov et al. (2003) [57], and is defined as a depletion in the intensity of nighttime irregular pulsations from the magnetosphere. This phenomenon is not well recognized, even in the academic circles; however, they suggested that this effect is due to lower ionospheric turbulences [57,58], just like subionospheric VLF/LF perturbation [10–14]. We demonstrate a method of analyzing ULF depression here. The daily value of absolute depression, Dep_h , in the total horizontal component of ULF magnetic field variations is calculated as follows:

$$Dep_h = \frac{1}{\langle F_h^2 \rangle_{\Delta T}} \quad (2)$$

where we have the squared output signal ($F_h = G$), observed using a sensor in any frequency band averaged over the local night interval $\Delta T = 01\text{--}05$ JST(LT) of four hours, as already described in the previous subsection.

4. ULF Observational Results

4.1. ULF Lithospheric Radiation

Figure 2 illustrates the plots of the ULF analysis results from the two months around the date of the 2016 Fukushima EQ. The frequency is 0.01–0.03 Hz, and the ULF effect is most significant after checking the results at different frequencies. The top panel illustrates the evolution in the geomagnetic activity of Kp (in blue) (though a detailed consideration of geomagnetic activities (Kp and Dst) has already been carried out in [68–70]) and the local seismicity at Kakioka (KIs) (denoted by yellow stars). The second and third panels refer to G and Z, respectively, and the fourth panel refers to the polarization Z/G. The bottom panel is the result of magnetic field depression, Dep (or Deph). Vertical red broken lines refer to the occurrence times of EQs.

A comparison of the temporal evolution of the horizontal component (G) with that of geomagnetic activity expressed via the Kp index suggests some similarity; we can find periods of an enhanced G component when the Kp index is increased. Of course, this parallelism is very partial, which means that the temporal behavior of the ULF horizontal magnetic field observed on the ground has a reasonable dependence on the geomagnetic activity (i.e., the space weather conditions). On the other hand, a comparison of the temporal evolutions of the Z component and Kp index indicates that the Z component is only slightly dependent on the Kp index with much lower intensity than G component. Taking into account this tendency, Hayakawa et al. (1996) [49] proposed a new physical parameter, “polarization”, defined as the ratio of the power of the vertical component to that of horizontal component, which was found to be extremely effective in identifying seismogenic ULF radiation from other general geomagnetic variations, such as geomagnetic pulsations [35–38,40–42,56]. The fourth panel refers to the temporal variation of this polarization, Z/G. The normal value of polarization is considerably below unity, as suggested by Hayakawa et al. (1996) [49], but we have found that the polarization exhibited a rather broad maximum (approaching and/or exceeding unity) from 14 to 20 November (7 days to 1 day before the EQ), and another single peak on 7 November 2016. The later broad maximum in a highly geomagnetically quiet period is likely to be a precursor to an EQ, but we wonder whether the sharp peak on 7 November is related to this EQ, or is related to a previous EQ (11/11/16) in the Miyagi prefecture (which is more likely). Those peaks in polarization are found to accompany subtle amplitudes, so the seismogenic ULF radiation

must be very weak in amplitude, which is likely due to the large epicentral distance of about 200 km (as compared with the previous ULF review paper) [50–53]. According to the empirical formula in Section 2, we have found that the threshold distance for the detection of seismogenic radiation for this EQ magnitude is 116 km, which is a little bit smaller than the real epicentral distance of 200 km.

4.2. ULF Depression Effect

We observed the bottom panel on ULF depression effect regarding this EQ. Two significant peaks in the ULF depression effect on 6–8 November and 20 November 2016 are noticeable. Both the parameters of polarization (as discussed in Section 4.1) and this ULF depression include the same denominator of the total horizontal component (G); thus, it is reasonable that the temporal behavior of both parameters shows a high similarity, but with slight shift in their temporal evolutions. However, we know that the ULF depression exhibits a sharp peak, as summarized in Section 1. Because the normal level of Dep is well below 10 in a.u., the peak in the ULF depression effect on 20 November (just one day before the EQ) is highly likely to be associated with our EQ, as a clear precursor to the EQ, because the lead time of ULF depression is around a few days. This is very consistent with the summary in Section 2, and also in [29]. We must then turn our attention to the second peak in ULF depression on 7 November 2016. It is likely that this ULF depression effect is related to another EQ on 11 November 2016, which occurred offshore of the Miyagi prefecture, with an epicentral distance of about 300 km. We will indicate the reasons that we concluded this. The first is that the lead time of the ULF depression before an EQ is around a few days (as indicated in Section 2, and also in [29]); therefore, it is very unlikely that this ULF depression is a consequence of the EQ on 21 November, 2016. Another is that we know that the range of the coverage of this ULF depression phenomenon is rather wide, much wider than that of the ULF lithospheric radiation; thus, an epicentral distance of 300 km is a possible range within which we may detect the effects of the Miyagi EQ.

5. A Comparison of the Observational Results with Previous Results

This EQ has been extensively investigated recently by our colleagues, using different physical parameters, and a few papers have already been published regarding the Fukushima EQ, including those of Asano et al. (2017) [68], Chowdhury et al. (2022) [69], and Biswas et al. (2023) [70]. Figure 3 is the summary of various seismogenic phenomena from the above publications together with the results in this paper. First, temporal evolutions in any phenomena in the lithosphere, such as ULF seismogenic radiation, are plotted at the bottom, in which ULF (K) refers to the result at Kakioka [69], and ULF (A) indicates the result in this paper. Unfortunately, no data are available from atmospheric parameters such as AGW (atmospheric gravity wave) activity [26], and Earth surface parameters, such as atmospheric temperature, brightness temperature, surface latent heat flux (SLHF), outgoing longwave radiation (OLR), thermal infrared spectral range (TIR), aerosols, etc. [24], were not studied either. Perturbations in the lower ionosphere were studied in the paper by Asano et al. (2017) [68], with the use of subionospheric VLF/LF propagation anomalies. VLF(J) refers to anomalous days in the observation of subionospheric propagation in Japan; VLF(R) represents the corresponding results from the Russian observatory at Kamchatka (from Japanese VLF/LF transmitters). Anomalous days are indicated by a horizontal bar with arrows at both ends. Finally, the effects of ULF depression are indicated in the same way; ULF dep (K) is the ULF depression at Kakioka [69], while ULF dep (A) refers to Asahi. Finally, AGW activity in the stratosphere [28] was studied by Politis et al. (2022) [71] for this EQ, with the use of data from European Center for Medium-Range Weather Forecasts, and their results are included in Figure 3.

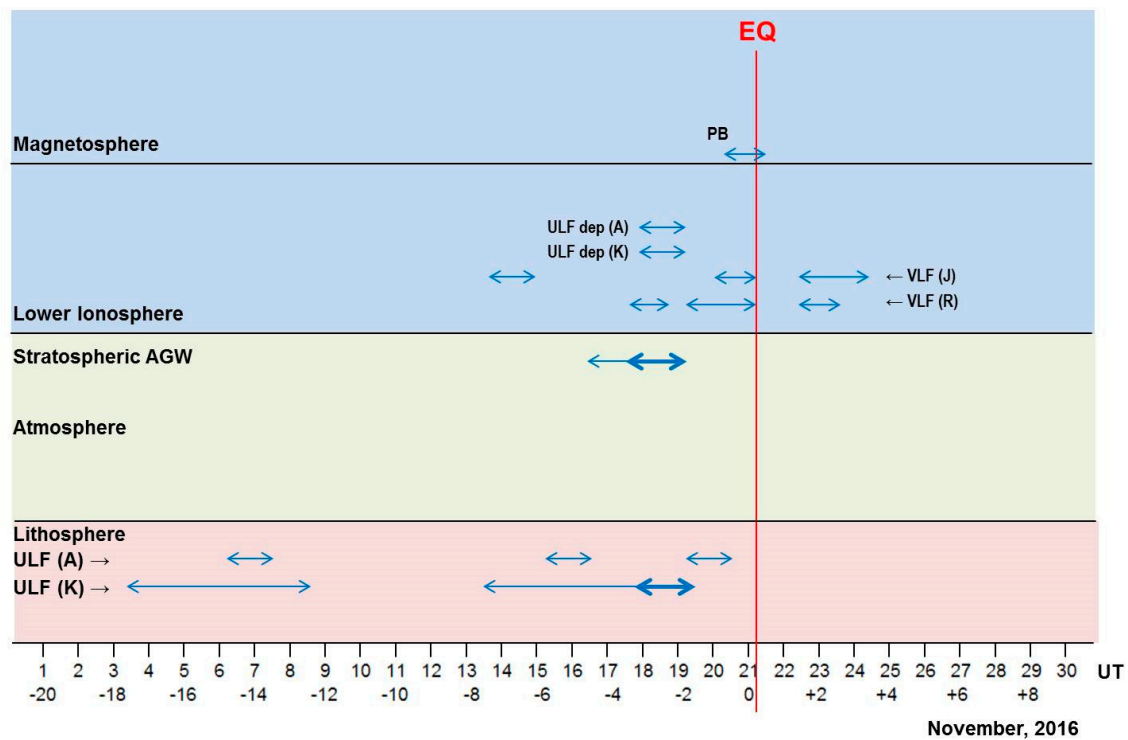


Figure 3. Summary of temporal evolutions of anomalies observed in different layers of the Earth. In the lithosphere, we indicate anomalies in ULF lithospheric radiation using horizontal lines with arrows at both ends, where K and A refer to Kakioka and Asahi, respectively. The thick part for Kakioka indicates the strongest intensity. The stratospheric AGW activity is presented in the same way, but the thick part indicates the highest activity. In the lower ionosphere, anomalies found using two independent methods are given; these are VLF anomalies, as observed in Japan (J) and Russia (R), and ULF depression anomalies (K and A). Finally, the PBs (particle bursts) were observed on the day of the EQ. The vertical red line represents the day of the EQ.

Herein, we tried to study the mechanism of LAIC. The initial agent of this LAIC process is definitely located in the bottom layer of lithosphere. As is shown in the summary plot of Figure 3, lithospheric radiation, as detected at Kakioka (closer to the EQ epicenter than Asahi), occurred mainly during the two time periods of 4–8 November (or 17–13 days before the EQ) and 14–19 November (7–2 days before the EQ) 2016, within the whole analysis period. This means that some electric currents must have been generated in the lithosphere due to a self-organized process during the EQ preparation phase [72,73]. Even though several hypotheses have been proposed, including the electro-kinetic effect, microfracturing effect, etc. [74–81], seismogenic ULF emissions are believed to originate from the local zones of EQs; this is reinforced by suggestions that mechanical deformation or microfracturing in the looming focal zones may give rise to pre- or co-seismic ULF emissions. Concerning the ULF radiation at Asahi station, we can see in Figure 3 that the occurrence of ULF radiation is well overlapped with periods of ULF radiation at Kakioka, but only in limited time periods on 7, 15, and 20 November 2016. This difference in temporal behavior at two stations is easily explained by the larger epicentral distance (by about 50 km) at Asahi.

Next, we summarize the results on perturbations in the lower ionosphere, using two “independent” methods of subionospheric VLF/LF propagation anomalies, and the ULF depression effect. As seen in Figure 3, the lower ionosphere is perturbed, as detected by VLF/LF propagation anomalies only just around the time of our target Fukushima EQ. At night, using Japanese data, we detected VLF/LF anomalies on 14–15 and 21 November (as precursory effects) and also 23 and 24 November (as after effects). Within the Russian data, we were able to detect VLF/LF propagation anomalies on 18, 19–20 November

(prior to the EQ) and also on 23 November (as a post-seismic effect). Of course, there is a possibility that those post-EQ events are a precursor to the subsequent aftershock of this EQ on 23 November. Recently, Kundu et al. (2023) [82] have found that the seismogenic ionospheric perturbation (as found by our multi-stationed Japanese VLF data) seems to be rather inhomogeneous in its spatial distribution, which might result in a small difference in the VLF anomalous days in the same period of time for different propagation paths, as observed in Figure 3. On the other hand, the ULF depression effects, are identified as a signature of lower ionospheric perturbation [83], are clearly seen on exactly the same day (20 November), just one day before the EQ, at both the stations of Kakioka and Asahi. Taking into account all these phenomena, we can conclude that the lower ionosphere is highly likely to be perturbed just around the time of the EQ, but mainly before the EQ.

Closely related to lower ionospheric perturbations, the AGW activity in the stratosphere has been examined by Politis et al. (2022) [71], who found that the AGW activity was very much enhanced on 18 and 19 November, as a precursor to this EQ, as can be seen in Figure 3.

Finally, the last phenomenon of particle precipitation was observed aboard a satellite [70], which indicated the particle precipitation on the day of the EQ, as shown in Figure 3.

We may now discuss the mechanism of LAIC process by comparing the temporal evolutions of different seismogenic phenomena, as shown in Figure 3. The mechanism of the LAIC process has been studied extensively over the last ten years, and a few hypotheses have already been proposed (e.g., [84–93]). As proposed in the work of Hayakawa et al. (2004) [84], the first is the so-called “chemical” channel; the emanation of radioactive radon and/or gases plays the main role, leading to the modification of atmospheric conductivity and the generation of an electric field, thereby prompting variation in the ionospheric plasma density [85–88]. The second channel is “acoustic”, in which atmospheric oscillations including atmospheric gravity waves (AGWs) and acoustic waves are excited by the precursory deformation of ground motion and/or fluctuations in gas emanation, which propagate upwards to the lower and upper ionosphere and lead to a perturbation in the ionosphere [89–91]. The third is the “electromagnetic” channel [92], wherein electromagnetic waves generated in the lithosphere in any frequency range propagate upwards into the ionosphere and magnetosphere, inducing particle precipitation into the upper atmosphere due to wave–particle interactions in the magnetosphere. Finally, a fourth “electrostatic” channel is proposed, based on the laboratory experiments, in which positive holes are generated when the ground of our interest is stressed by the accumulated pressure [93]. These processes have been discussed extensively by different authors (e.g., [24–28]), but the above hypotheses have not been evidenced by any observational data. Essentially, the first and fourth channels are based on the formation of an electric field in the atmosphere, but there is a serious problem presented by the extremely low efficiency of the transmission of the atmospheric electric field into the ionosphere [94,95], even though radon emanation is known to be a precursor to EQs [96]. On the other hand, recently, a lot of evidence has been accumulated on the AGW channel, using different kinds of observations [97–102].

When we observed the first interval of ULF radiation, as shown in Figure 3 (on 4–8 November), we could not find any effects on the ionospheric height. This may suggest that the current systems induced in the lithosphere during the EQ’s preparation (of which the most promising is electro-kinetic effect) have no effect on the ionosphere; meanwhile, when we observed the second interval of 14–19 November for the detection of ULF lithospheric radiation, the situation in the upper region we found to be completely different from the first interval, because the lower ionosphere is considerably perturbed, not only before the EQ, but also after the EQ. The days of ionospheric perturbations, as detected by subionospheric VLF/LF signals, are 14–15, 18, and 20–21 November, as a precursory signature of the EQ. The ionospheric perturbations after the EQ are supposed to be either the after-effect of this EQ, or a precursory effect of the aftershock of this EQ on 23 November. The much more obvious precursor of the ULF depression effects, as observed at both ULF

stations of Kakioka and Asahi, was completely coincident in time and on 19 November, two days before the EQ (this being consistent with the general behavior summarized in Section 2), which may suggest that the ionosphere was most disturbed on this day. Appearing to support the generation of lower ionospheric perturbation, Politis et al. [71] found that AGW activity began to increase on 17 November, and was very much enhanced on 18 and 19 November, as is summarized in Figure 3. These dates are coincident with those of the lower ionospheric VLF/LF perturbations, and also with the day of maximum ULF radiation detected at Kakioka. We normally observe VLF/LF ionospheric disturbances a few days to about one week before an EQ [12,13], so the perturbations on 14–15 and 18 November are certain to be a precursor to this Fukushima EQ. Further, the ionospheric perturbations on 18 and 20–21 November are also likely to be precursors to this EQ. The comparison of the temporal behavior of VLF/LF propagation anomalies and the stratospheric AGW activities suggests that the AGW hypothesis is a likely agent of the LAIC process. However, in order to support this hypothesis, it is necessary for us to investigate whether there must be any fluctuations present, in the AGW frequency range, in the surface parameters including surface deformation [100–102], and surface meteorological parameters such as air temperature, pressure, etc. We finally comment on another possibility: that the ionospheric perturbation on 21 November might be correlated with the PB (particle precipitation) on the date of EQ, as a consequence of particle precipitation from wave–particle interactions in the magnetosphere [92]. More information on the upper ionosphere (F region) is required, supported by data from GPS TEC and satellite observations; this will be the basis of our future work.

Based on all of these considerations, it seems we can identify a chain-like tendency of seismogenic effects, initially in the lithosphere and propagating upwards into the lower ionosphere (with some delay). In this context, the AGW hypothesis seems plausible as a mechanism of the LAIC process for this EQ; however, we are not ready to conclude which channel of the LAIC process (the AGW or electromagnetic channel) is in operation for this Fukushima EQ. In order to gain deeper understanding, we need to acquire extensive information on the Earth surface parameters and on stratospheric AGW activity in the near future.

6. Conclusions

We have presented the first report on our ULF observations at a new ULF station at Asahi, in the Chiba prefecture; we hope to predict any possible big EQs in the Tokyo district based on observations made at Asahi. We are threatened by the prospect of the first huge EQ since the 1923 Tokyo EQ. In this paper, we selected the 2016 November Fukushima EQ, with huge magnitude of 7.4, as a case study, and have presented the significant EQ precursors of ULF lithospheric radiation and the ULF depression effect, using Asahi ULF data. Furthermore, in order to confirm a possible relationship between the observed anomaly and the EQ, we have to carry out a critical analysis [14,73] and/or artificial intelligence (AI) (e.g., with machine learning) analysis [103]; this will feature in our future work.

These ULF results have been compared with our previous observational results on different physical parameters, and we have found that a variety of seismogenic anomalies take place in different layers of the Earth; they also tend to be concentrated in the temporal interval just around the occurrence of the EQ, but mainly prior to the EQ, indicating the presence of a pre-EQ preparation critical phase. In future, we plan to study the upper ionospheric condition, in order to enrich the information on the LAIC process. We have tried to better understand the mechanism of the LAIC process, but we are not yet ready to present a conclusion regarding the LAIC process of this EQ. In order to gain full understanding of the LAIC process of this EQ, we need to study more physical parameters, especially those on and above the Earth's surface.

Author Contributions: Conceptualization, M.H., observation, H.Y. and Y.H.; analysis and discussion, A.S. and Y.H.; writing, review and editing, M.H. All authors have read and agreed to the published version of the manuscript.

Funding: This research received no external funding.

Informed Consent Statement: Not applicable.

Data Availability Statement: Data can be available upon the request of any scientist.

Acknowledgments: The observation of ULF waves at Asahi was initiated in 2014 as a collaborative work between Hi-SEM and Fuji DR Security Co., Ltd., and we thank the staffs of Fuji DR Security Co., Ltd. for their support. Further, we would like to dedicate this paper to the late A. Schekotov (passed away in April, 2023) for his continued excellent contribution to Seismo Electromagnetics studies.

Conflicts of Interest: The authors declare no conflict of interests.

References

1. Hayakawa, M.; Molchanov, O. (Eds.) *Seismo Electromagnetics: Lithosphere-Atmosphere-Ionosphere Coupling*; Terrapub: Tokyo, Japan, 2002; p. 477.
2. Pulinets, S.; Boyarchuk, K. *Ionospheric Precursors of Earthquakes*; Springer: Berlin/Heidelberg, Germany, 2004; p. 315.
3. Molchanov, O.A.; Hayakawa, M. *Seismo-Electromagnetics and Related Phenomena: History and Latest Results*; TERRAPUB: Tokyo, Japan, 2008; p. 189.
4. Hayakawa, M. *Earthquake Prediction with Radio Techniques*; John Wiley & Sons: Singapore, 2015; p. 294.
5. Sorokin, V.; Chemyrev, V.V.; Hayakawa, M. *Electrodynamic Coupling of Lithosphere-Atmosphere-Ionosphere of the Earth*; Nova Science Pub. Inc.: New York, NY, USA, 2015; p. 326.
6. Ouzounov, D.; Pulinets, S.; Hattori, K.; Taylor, P. (Eds.) *Pre-Earthquake Processes: A Multidisciplinary Approach to Earthquake Prediction Studies*; AGU (American Geophysical Union) Geophysical Monograph, 234; Wiley: New York, NY, USA, 2018; p. 365.
7. Conti, L.; Picozza, P.; Sotgiu, A. A critical review of ground-based observations of earthquake precursors. *Front. Earth Sci.* **2021**, *9*, 676766. [[CrossRef](#)]
8. Picozza, P.; Conti, L.; Sotgiu, A. Looking for earthquake precursors from space: A critical review. *Front. Earth Sci.* **2021**, *9*, 676775. [[CrossRef](#)]
9. Chen, H.; Han, P.; Hattori, K. Recent advances and challenges in the seismo-electromagnetic study: A brief review. *Remote Sens.* **2022**, *14*, 5893. [[CrossRef](#)]
10. Hayakawa, M. Probing the lower ionosphere by means of subionospheric VLF propagation. *Earthq. Sci.* **2011**, *24*, 609–637. [[CrossRef](#)]
11. Hayakawa, M.; Asano, T.; Rozhnoi, A.; Solovieva, M. Very-low- and low-frequency sounding of ionospheric perturbations and possible association with earthquakes. In *Pre-Earthquake Processes: A Multidisciplinary Approach to Earthquake Prediction Studies*; Ouzounov, D., Pulinets, S., Hattori, K., Taylor, P., Eds.; AGU Geophysical Monograph; Wiley: New York, NY, USA, 2018; Chapter 16; pp. 277–304.
12. Hayakawa, M.; Kasahara, Y.; Nakamura, T.; Muto, F.; Horie, T.; Maekawa, S.; Hobara, Y.; Rozhnoi, A.A.; Solovieva, M.; Molchanov, O.A. A statistical study on the correlation between lower ionospheric perturbations as seen by subionospheric VLF/LF propagation and earthquakes. *J. Geophys. Res.* **2010**, *115*, A09305. [[CrossRef](#)]
13. Rozhnoi, A.; Solovieva, M.S.; Molchanov, O.A.; Hayakawa, M. Middle latitude LF (40 kHz) phase variations associated with earthquakes for quiet and disturbed geomagnetic conditions. *Phys. Chem. Earth* **2004**, *29*, 589–598. [[CrossRef](#)]
14. Politis, D.Z.; Potirakis, S.M.; Contoyiannis, Y.F.; Biswas, S.; Sasmal, S.; Hayakawa, M. Statistical and criticality analysis of the lower ionosphere prior to the 30 October 2020 Samos (Greece) earthquake (M6.9), based on VLF electromagnetic propagation data as recorded by a new VLF/LF receiver installed in Athens (Greece). *Entropy* **2021**, *23*, 676. [[CrossRef](#)]
15. Liu, J.Y. Earthquake precursors observed in the ionospheric F-region. In *Electromagnetic Phenomena Associated with Earthquakes*; Hayakawa, M., Ed.; Transworld Research Network: Trivandrum, India, 2009; pp. 187–204.
16. Liu, J.Y.; Hattori, K.; Chen, Y.I. Application of total electron content derived from the global navigation satellite system for detecting earthquake precursors. In *Pre-Earthquake Processes: A Multidisciplinary Approach to Earthquake Prediction Studies*; Ouzounov, D., Pulinets, S., Hattori, K., Taylor, P., Eds.; AGU Geophysical Monograph; Wiley: New York, NY, USA, 2018; pp. 305–317.
17. Parrot, M.; Li, M. Statistical analysis of the ionospheric density recorded by the DEMETER satellite during seismic activity. In *Pre-Earthquake Processes: A Multidisciplinary Approach to Earthquake Prediction Studies*; Ouzounov, D., Pulinets, S., Hattori, K., Taylor, P., Eds.; AGU Geophysical Monograph; Wiley: New York, NY, USA, 2018; pp. 319–328.
18. Kon, S.; Nishihashi, M.; Hattori, K. Ionospheric anomalies possibly associated with M > 6.0 earthquakes in the Japan area during 1998–2010: Case studies and statistical study. *J. Asian Earth Sci.* **2011**, *41*, 410–420. [[CrossRef](#)]
19. Li, M.; Shen, X.; Parrot, M.; Zhang, X.; Zhang, Y.; Yu, C.; Yan, R.; Liu, D.; Lu, H.; Guo, F.; et al. Primary joint statistical seismic influence on ionospheric parameters recorded by the CSES and DEMETER satellites. *J. Geophys. Res. Space Phys.* **2020**, *125*, e2020JA028116. [[CrossRef](#)]

20. Zeng, L.; Yan, R.; Parrot, M.; Zhu, K.; Zhima, Z.; Liu, D.; Xu, S.; Lv, F.; Shen, X. Statistical research on seismo-ionospheric ion density enhancements observed via demeter. *Atmosphere* **2022**, *13*, 1252. [[CrossRef](#)]
21. Marchetti, D.; De Santis, A.; D'Arcangelo, S.; Poggio, F.; Piscini, A.; Campuzano, A.; Werneck, V. Pre-earthquake chain processes detected from ground to satellite altitude in preparation of the 2016–2017 seismic sequence in Central Italy. *Remote Sens. Environ.* **2019**, *229*, 93–99. [[CrossRef](#)]
22. De Santis, A.; Marchetti, D.; Spogli, L.; Cianchini, G.; Pavon-Carrasco, F.J.; Franceschi, G.D.; Di Giovambattista, R.; Perrone, L.; Qamili, E.; Cesaroni, C.; et al. Magnetic field and electron density data analysis from Swarm satellites searching for ionospheric effects by great earthquakes: 12 case studies from 2014 to 2016. *Atmosphere* **2019**, *10*, 371. [[CrossRef](#)]
23. He, Y.; Zhao, X.; Yang, D.; Wu, Y.; Li, Q. A study to investigate the relationship between ionospheric disturbances and seismic activity based on Swarm satellite data. *Phys. Earth Planet Inter.* **2021**, *323*, 106826. [[CrossRef](#)]
24. Ouzounov, D.; Pulinet, S.; Davidenko, D.; Rozhnoi, A.; Solovieva, M.; Fedun, V.; Dwiredi, B.N.; Rybin, A.; Kafatos, M.; Taylor, P. Transient effects in atmosphere and ionosphere preceding the 2015 M7.8 and M7.3 Gorkha-Nepan earthquakes. *Front. Earth Sci.* **2021**, *9*, 757358. [[CrossRef](#)]
25. Sasmal, S.; Chowdhury, S.; Kundu, S.; Politis, D.Z.; Potirakis, S.M.; Balasis, G.; Hayakawa, M.; Chakrabarti, S.K. Pre-seismic irregularities during the 2020 Samos (Greece) earthquake (M = 6.9) as investigated from multi-parameter approach by ground and space-based techniques. *Atmosphere* **2021**, *12*, 1059. [[CrossRef](#)]
26. Hayakawa, M.; Izutsu, J.; Schekotov, A.; Yang, S.S.; Solovieva, M.; Budilova, E. Lithosphere-atmosphere-ionosphere coupling effects based on multiparameter precursor observations for February–March 2021 earthquakes (M~7) in the offshore of Tohoku area of Japan. *Geosciences* **2021**, *11*, 481. [[CrossRef](#)]
27. Hayakawa, M.; Schekotov, A.; Izutsu, J.; Yang, S.S.; Solovieva, M.; Hobar, Y. Multi-parameter observation of seismogenic phenomena related to the Tokyo earthquake (M = 5.9) on 7 October 2021. *Geosciences* **2022**, *12*, 265. [[CrossRef](#)]
28. Ghamry, E.; Mohamed, E.K.; Sekertikin, A.; Fathy, A. Investigation of multiple earthquake precursors before large earthquakes: A case study of 25 April 2015 Nepal. *J. Atmos. Sol.-Terr. Phys.* **2023**, *242*, 105982. [[CrossRef](#)]
29. Hayakawa, M.; Schekotov, A.; Izutsu, J.; Nickolaenko, A.P.; Hobar, Y. Seismogenic ULF/ELF wave phenomena: Recent advances and future perspectives. *Open J. Earthq. Res.* **2023**, *12*, 45–113. [[CrossRef](#)]
30. Hayakawa, M.; Schekotov, A.; Izutsu, J.; Nickolaenko, A.P. Seismogenic effects in ULF/ELF/VLF electromagnetic waves. *Int. J. Electron. Appl. Res.* **2019**, *6*, 1–86.
31. Han, P.; Hattori, K.; Hirokawa, M.; Zhuang, J.; Chen, C.H.; Febriani, F.; Yamaguchi, H.; Yoshino, C.; Liu, J.Y.; Yoshida, S. Statistical analysis of ULF seismomagnetic phenomena at Kakioka, Japan, during 2001–2010. *J. Geophys. Res. Space Phys.* **2014**, *119*, 4998–5011. [[CrossRef](#)]
32. Han, P.; Hattori, K.; Hirrooka, M.; Zhuang, J.; Chen, C.H.; Febriani, F.; Yamaguchi, H.; Yoshino, C.; Liu, J.Y.; Yoshida, S. Evaluation of ULF seismo-magnetic phenomena in Kakioka, Japan by using Molchan's error diagram. *Geophys. J. Int.* **2017**, *208*, 482–490. [[CrossRef](#)]
33. Masci, F.; Thomas, J. Are there any new findings in the research for ULF magnetic precursors to earthquakes? *J. Geophys. Res. Space Phys.* **2015**, *120*, 10289–10304. [[CrossRef](#)]
34. Schekotov, A.; Hayakawa, M. *ULF/ELF Electromagnetic Phenomena for Short-term Earthquake Prediction*; LAP Lambert Academic Publishing: Beau Bassin, Mauritius, 2017; p. 102.
35. Singh, V.; Hobar, Y. Simultaneous study of VLF/ULF anomalies associated with earthquakes in Japan. *Open J. Earthq. Res.* **2020**, *9*, 201–215. [[CrossRef](#)]
36. Yusof, K.A.; Abdallah, M.; Hamid, N.S.A.; Ahadi, S. Correlations between earthquake properties and characteristics of possible ULF geomagnetic precursor over multiple earthquakes. *Universe* **2022**, *7*, 20. [[CrossRef](#)]
37. Stanica, D.A.; Stanica, D. ULF pre-seismic geomagnetic anomalous 2017, A signal related to Mw8.1 offshore Chiapas earthquake, Mexico on 8 September 2017. *Entropy* **2019**, *21*, 29. [[CrossRef](#)]
38. Zhou, H.; Yan, F.; Wang, J.; Luo, Q.; Jin, T. Study on the ULF geomagnetic field generated by earth currents relating to large earthquakes. *Radio Sci.* **2019**, *56*, e2019RS006992. [[CrossRef](#)]
39. Warden, S.; MacLean, L.; Lemon, J.; Schneider, D. Statistical analysis of pre-earthquake electromagnetic anomalies in the ULF range. *J. Geophys. Res. Space Phys.* **2020**, *125*, e2020JA027955. [[CrossRef](#)]
40. Feng, L.; Qu, R.; Ji, Y.; Zhu, W.; Zhu, Y.; Feng, Z.; Fan, W.; Guan, Y.; Xie, C. Multistationary geomagnetic vertical intensity polarization anomalies for predicting $M \geq 6$ earthquakes in Qinghai, China. *Appl. Sci.* **2022**, *12*, 8888. [[CrossRef](#)]
41. Xiang, C.; Li, M.; Ma, Z.; Teng, C.; Li, Z.; Shao, Z. Ultra-low frequency electromagnetic emissions registered during the 21 May 2021 Yangbi Ms 6.4 earthquake in China. *Nat. Sci.* **2022**, *14*, 1–12. [[CrossRef](#)]
42. Bulusu, J.; Arora, K.; Singh, S.; Edara, A. Simultaneous electric, magnetic and ULF anomalies associated with moderate earthquakes in Kumaun Himalaya. *Nat. Hazards* **2023**, *116*, 3925–3955. [[CrossRef](#)]
43. Heavin, W.D.; Kappler, K.; Yang, L.; Fan, M.; Hickey, J.; Lemon, J.; MacLean, L.; Bleier, T.; Riley, P.; Schneider, D. Case-concept study on a decade of ground-based magnetometers in California reveals modest signal 24–72 h prior to earthquakes. *J. Geophys. Res. Solid Earth* **2022**, *127*, e2022JB024109. [[CrossRef](#)]
44. Kasdi, A.S.; Bouzid, A.; Hamoudi, M.; Abtout, A. Singular spectral analysis applied to magnetotelluric time series collected at Medea geomagnetic observatory (Algeria)- an attempt to discriminate earthquake-related signal. *Arab. J. Geosci.* **2022**, *15*, 1178. [[CrossRef](#)]

45. Moore, G.W. Magnetic disturbances preceding the 1964 Alaska earthquake. *Nature* **1964**, *203*, 508–509. [[CrossRef](#)]
46. Fraser-Smith, A.C.; Bernardi, A.; McGill, P.R.; Ladd, M.E.; Helliwell, R.A.; Villard, O.G., Jr. Low-frequency magnetic field measurements near the epicenter of the Ms 7.1 Loma Prieta earthquake. *Geophys. Res. Lett.* **1990**, *17*, 1465–1468. [[CrossRef](#)]
47. Kopytenko, Y.A.; Matiashvily, T.G.; Voronov, P.M.; Kopytenko, E.A.; Molchanov, O.A. Detection of ULF emission connected with the Spitak earthquake and its aftershock activity based on geomagnetic pulsations data at Dusheti and Vardziya observatories. *Phys. Earth Planet. Inter.* **1990**, *77*, 85–95. [[CrossRef](#)]
48. Molchanov, O.A.; Kopytenko, Y.A.; Voronov, P.M.; Kopytenko, E.A.; Matiashvily, T.G.; Fraser-Smith, A.C.; Bernardi, A. Results of ULF magnetic field measurements near the epicenters of the Spitak (Ms = 6.9) and Loma Prieta (Ms = 7.1) earthquakes: Comparative analysis. *Geophys. Res. Lett.* **1992**, *19*, 1495–1498. [[CrossRef](#)]
49. Hayakawa, M.; Kawate, R.; Molchanov, O.A.; Yumoto, K. Results of ultra-low-frequency magnetic field measurements during the Guam earthquake of 8 August 1993. *Geophys. Res. Lett.* **1996**, *23*, 241–244. [[CrossRef](#)]
50. Hayakawa, M.; Hattori, K.; Ohta, K. Monitoring of ULF (ultra low frequency) geomagnetic variations associated with earthquakes. *Sensors* **2007**, *7*, 1108–1122. [[CrossRef](#)]
51. Hayakawa, M.; Hobara, Y.; Ohta, K.; Hattori, K. The ultra-low-frequency magnetic disturbances associated with earthquakes. *Earthq. Sci.* **2011**, *24*, 523–534. [[CrossRef](#)]
52. Hattori, K. ULF geomagnetic changes associated with large earthquakes. *Terr. Atmos. Ocean. Sci.* **2004**, *15*, 329–360. [[CrossRef](#)]
53. Hattori, K. ULF geomagnetic changes associated with earthquakes. In *Earthquake Prediction Studies: Seismo Electromagnetics*; Hayakawa, M., Ed.; TERRAPUB: Tokyo, Japan, 2013; pp. 129–152.
54. Shrivastava, A. Are pre-seismic ULF electromagnetic emissions as a reliable earthquake prediction? *Curr. Sci.* **2014**, *107*, 596–600.
55. Piriye, R. Electromagnetic earthquake precursory signatures in the ULF range: Perspectives of the studies. *Geophysics* **2021**, *1*, 48–57. [[CrossRef](#)]
56. Currie, J.L.; Waters, C.L. On the use of geomagnetic indices and ULF waves for earthquake precursor signatures. *J. Geophys. Res. Space Phys.* **2014**, *119*, 992–1003. [[CrossRef](#)]
57. Molchanov, O.A.; Schekotov, A.Y.; Fedorov, E.N.; Belyaev, G.G.; Gordeev, E.E. Preseismic ULF electromagnetic effect from observation at Kamchatka. *Nat. Hazards Earth Syst. Sci.* **2003**, *3*, 1–7. [[CrossRef](#)]
58. Molchanov, O.A.; Schekotov, A.Y.; Fedorov, E.; Belyaev, G.; Solovieva, M.S.; Hayakawa, M. Preseismic ULF effect and possible interpretation. *Ann. Geophys.* **2004**, *47*, 119–131.
59. Schekotov, A.; Molchanov, O.; Hattori, K.; Fedorov, E.; Gladyshev, V.A.; Belyaev, G.G.; Chebrov, V.; Sinitsin, V.; Gordeev, E.; Hayakawa, M. Seismo-ionospheric depression of the ULF geomagnetic fluctuations at Kamchatka and Japan. *Phys. Chem. Earth* **2006**, *31*, 313–318. [[CrossRef](#)]
60. Schekotov, A.; Fedorov, E.; Hobara, Y.; Hayakawa, M. ULF magnetic field depression as a possible precursor to the 2011/3.11 Japan earthquake. *J. Atmos. Electr.* **2013**, *33*, 41–51. [[CrossRef](#)]
61. Hayakawa, M.; Schekotov, A.; Fedorov, E.; Hobara, Y. On the ultra-low-frequency magnetic field depression for three huge oceanic earthquakes in Japan and in the Kurile islands. *Earth Sci. Res.* **2013**, *2*, 33–42. [[CrossRef](#)]
62. Hayakawa, M.; Rozhnoi, A.; Solovieva, M.; Hobara, Y.; Ohta, K. The lower ionospheric perturbation as a precursor to the 11 March 2011 Japan earthquake, Geomatics. *Nat. Hazards Risk* **2013**, *4*, 275–287. [[CrossRef](#)]
63. Schekotov, A.; Chebrov, D.; Hayakawa, M.; Belyaev, G.; Berseneva, N. Short-term earthquake prediction in Kamchatka using low-frequency magnetic fields. *Nat. Hazards* **2020**, *100*, 735–755. [[CrossRef](#)]
64. Schekotov, A.; Fedorov, E.; Molchanov, O.A.; Hayakawa, M. Low frequency electromagnetic precursors as a prospect for earthquake prediction. In *Earthquake Prediction Studies: Seismo Electromagnetics*; Hayakawa, M., Ed.; TERRAPUB: Tokyo, Japan, 2013; pp. 81–99.
65. Dobrovolsky, I.R.; Zubkov, S.I.; Miachkin, V.I. Estimation of the size of earthquake preparation zones. *Pure Appl. Geophys.* **1998**, *117*, 1025–1044. [[CrossRef](#)]
66. Ruzhin, Y.Y.; Depueva, A.K. Seismoprecursors in space as plasma and wave anomalies. *J. Atmos. Electr.* **1996**, *16*, 271–288. [[CrossRef](#)]
67. Bowman, D.D.; Ouillon, G.; Sammis, C.G.; Sornett, A.; Sornett, D. An observational test of the critical earthquake concept. *J. Geophys. Res. Solid Earth* **1998**, *103*, 24359–24372. [[CrossRef](#)]
68. Asano, T.; Rozhnoi, A.; Solovieva, M.; Hayakawa, M. Characteristic variations of VLF/LF signals during a high seismic activity in Japan in November 2016. *Open J. Earthq. Res.* **2017**, *6*, 204–215. [[CrossRef](#)]
69. Chowdhury, S.; Kundu, S.; Gosh, S.; Hayakawa, M.; Schekotov, A.; Potirakis, S.M.; Chakrabarti, S.K. Direct and indirect evidence of pre-seismic electromagnetic emissions associated with two large earthquakes in Japan. *Nat. Hazards* **2022**, *112*, 2403–2432. [[CrossRef](#)]
70. Biswas, S.; Kundu, S.; Sasmal, S.; Politis, D.Z.; Potirakis, S.M.; Hayakawa, M. Preseismic perturbations and their inhomogeneity as computed from ground- and space-based investigation during the 2016 Fukushima earthquake. *J. Sens.* **2023**, *2023*, 7159204. [[CrossRef](#)]
71. Politis, Z.; Potirakis, S.M.; Kundu, S.; Chowdhury, S.; Sasmal, S.; Hayakawa, M. Critical dynamics in stratospheric potential energy variations prior to significant ($M \geq 6.7$) earthquakes. *Symmetry* **2022**, *14*, 1939. [[CrossRef](#)]

72. Hayakawa, M.; Schekotov, A.; Potirakis, P.M.; Eftaxias, K. Critical features in ULF magnetic fields prior to the 2011 Tohoku earthquake. *Proc. Jpn. Acad. Ser. B Phys. Biol. Sci.* **2015**, *91*, 25–30. [[CrossRef](#)]
73. Potirakis, P.M.; Eftaxias, K.; Schekotov, A.; Yamaguchi, H.; Hayakawa, M. Critical features in ultra-low frequency magnetic fields prior to the 2013 Kobe earthquake. *Ann. Geophys.* **2016**, *59*, S0317.
74. Mizutani, H.; Ishido, T. A new interpretation of magnetic field variation associated with Matsushiro earthquakes. *J. Geomag. Geoelectr.* **1976**, *28*, 179–188. [[CrossRef](#)]
75. Mizutani, H.; Ishiso, T.; Yokokura, S. Ohnishi, Electrokinetic phenomena associated with earthquakes. *Geophys. Res. Lett.* **1976**, *3*, 365–368. [[CrossRef](#)]
76. Fitterman, D.V. Theory of electrokinetic magnetic anomalies in faulted half-space. *J. Geophys. Res.* **1979**, *84*, 6031–6040. [[CrossRef](#)]
77. Fenoglio, M.A.; Johnston, M.J.S.; Byerlee, J.D. Magnetic and electric fields associated with changes in high pore pressure in fault zone -application to the Loma Prieta ULF emissions. *J. Geophys. Res. Solid Earth* **1995**, *100*, 12951–12958. [[CrossRef](#)]
78. Dudkin, F.; De Santis, A.; Korepanov, V. Active EM sounding for early warning of earthquakes and volcanic eruption. *Phys. Earth Planet. Inter.* **2003**, *139*, 187–195. [[CrossRef](#)]
79. Molchanov, O.A.; Hayakawa, M. Generation of ULF electromagnetic emissions by microfracturing. *Geophys. Res. Lett.* **1995**, *22*, 3091–3094. [[CrossRef](#)]
80. Tzanis, A.; Vallianatos, F. A.; Vallianatos, F. A physical model of electric earthquake precursors due to crack propagation and the motion of charged edge dislocations. In *Seismo Electromagnetics: Lithosphere-Atmosphere-Ionosphere Coupling*; Hayakawa, M., Molchanov, O.A., Eds.; TERRAPUB: Tokyo, Japan, 2002; pp. 117–130.
81. Surkov, V.; Molchanov, O.A.; Hayakawa, M. Pre-earthquake ULF electromagnetic perturbations as a result of inductive seismogenic phenomena during microfracturing. *J. Atmos. Sol.-Terr. Phys.* **2003**, *65*, 31–46. [[CrossRef](#)]
82. Kundu, S.; Chowdhury, S.; Ghosh, S.; Sasmal, S.; Politis, D.; Potirakis, S.M.; Yang, S.S.; Chakrabarti, S.K.; Hayakawa, M. Seismogenic anomalies in Atmospheric Gravity Waves observed from SABER/TIMED satellite during large earthquakes. *J. Sens.* **2022**, *2022*, 3201104. [[CrossRef](#)]
83. Sorokin, V.M.; Fedorov, E.N.; Schekotov, A.V.; Molchanov, O.A.; Hayakawa, M. Depression of the ULF pulsation related to ionospheric irregularities. *Ann. Geophys.* **2004**, *47*, 192–198. [[CrossRef](#)]
84. Hayakawa, M.; Molchanov, O.A.; NASDA/UEC Team. Summary report of NASDA's earthquake remote sensing frontier project. *Phys. Chem. Earth* **2004**, *29*, 617–625. [[CrossRef](#)]
85. Pulnits, S.; Ouzounov, D. Lithosphere-atmosphere-ionosphere coupling (LAIC) model—a unified concept for earthquake precursors validation. *J. Asian Earth Sci.* **2011**, *41*, 371–382. [[CrossRef](#)]
86. Sorokin, V.M.; Yaschenko, A.K.; Hayakawa, M. Formation mechanism of the lower-ionospheric disturbances by the atmospheric electric current over a seismic region. *J. Atmos. Sol.-Terr. Phys.* **2006**, *68*, 1260–1268. [[CrossRef](#)]
87. Sorokin, V.; Hayakawa, M. Plasma and electromagnetic effects caused by the seismic-related disturbances of electric current in the global circuit. *Mod. Appl. Sci.* **2014**, *8*, 61–83. [[CrossRef](#)]
88. Harrison, R.G.; Alpin, K.L.; Rycroft, M.J. Atmospheric electricity coupling between earthquake regions and the ionosphere. *J. Atmos. Sol.-Terr. Phys.* **2010**, *72*, 376–381. [[CrossRef](#)]
89. Molchanov, O.A.; Hayakawa, M.; Miyaki, K. VLF/LF sounding of the lower ionosphere to study the role of atmospheric oscillations in the lithosphere-ionosphere coupling. *Adv. Polar Up. Atmos. Res.* **2001**, *15*, 146–158.
90. Miyaki, K.; Hayakawa, M.; Molchanov, O.A. The role of gravity waves in the lithosphere—ionosphere coupling, as revealed from the subionospheric LF propagation data. In *Seismo Electromagnetics: Lithosphere—Atmosphere—Ionosphere Coupling*; TERRAPUB: Tokyo, Japan, 2002; pp. 229–232.
91. Hayakawa, M.; Kasahara, Y.; Nakamura, T.; Hobara, Y.; Rozhnoi, A.; Solovieva, M.; Molchanov, O.A.; Korepanov, V. Atmospheric gravity waves as a possible candidate for seismo-ionospheric perturbations. *J. Atmos. Electr.* **2011**, *31*, 129–140. [[CrossRef](#)]
92. Molchanov, O.A.; Mazhaeva, O.A.; Goliavin, A.N.; Hayakawa, M. Observations by the intercosmos-24 satellite of ELF-VLF electromagnetic emissions associated with earthquakes. *Ann. Geophys.* **1993**, *11*, 431–440.
93. Freund, F. Stress-activated positive hole charge carriers in rocks and the generation of pre-earthquake signals. In *Electromagnetic Phenomena Associated with Earthquakes*; Hayakawa, M., Ed.; Transworld Research Network: Trivandrum, India, 2009; pp. 41–96.
94. Denisenko, V.V. Estimate for the strength of the electric field penetration from the Earth's surface to the ionosphere. *Russ. J. Phys. Chem.* **2015**, *70*, 2251–2253.
95. Prokhorov, B.E.; Zolotov, O.V. Comment on “An improved coupling model for the lithosphere-atmosphere-ionosphere coupling system” by Kuo et al. (2014). *J. Geophys. Res. Space Phys.* **2017**, *122*, 4865–4868. [[CrossRef](#)]
96. Yasuoka, Y. Radon anomalies prior to earthquakes. In *The Frontier of Earthquake Prediction Studies*; Hayakawa, M., Ed.; Nihon-Senmontosho-Shuppan: Tokyo, Japan, 2012; pp. 410–427. (In Japanese)
97. Korepanov, V.; Hayakawa, M.; Yampolski, Y.; Lizunov, G. AGW as a seismo-ionospheric coupling responsible agent. *Phys. Chem. Earth Parts A/B/C* **2009**, *34*, 6–7, Special issue, Electromagnetic Phenomena Associated with Earthquakes and Volcanoes. Edited by Hayakawa, M.; Liu, J.Y.; Hattori, K.; Telesca, L. pp. 485–495. [[CrossRef](#)]
98. Hayakawa, M.; Kasahara, Y.; Endoh, T.; Hobara, Y.; Asai, S. The observation of Doppler shifts of subionospheric LF signal in possible association with earthquakes. *J. Geophys. Res.* **2012**, *117*, A09304. [[CrossRef](#)]

99. Nakamura, T.; Korepanov, V.; Kasahara, Y.; Hobara, Y.; Hayakawa, M. An evidence on the lithosphere-ionosphere coupling in terms of atmospheric gravity waves on the basis of a combined analysis of surface pressure, ionospheric perturbations and ground-based ULF variations. *J. Atmos. Electr.* **2013**, *33*, 53–68. [[CrossRef](#)]
100. Yang, S.S.; Asano, T.; Hayakawa, M. Abnormal gravity wave activity in the stratosphere prior to the 2016 Kumamoto earthquakes. *J. Geophys. Res. Space Phys.* **2019**, *124*, 1410–1425. [[CrossRef](#)]
101. Yang, S.S.; Hayakawa, M. Gravity wave activity in the stratosphere before the 2011 Tohoku earthquake as the mechanism of lithosphere-atmosphere-ionosphere coupling. *Entropy* **2020**, *22*, 110. [[CrossRef](#)]
102. Chen, C.H.; Sun, Y.Y.; Zhang, X.; Gao, Y.; Wang, F.; Lin, K.; Tang, C.C.; Huang, R.; Xu, R.; Liu, J.; et al. Resonant signals in the lithosphere-atmosphere-ionosphere coupling. *Sci. Rep.* **2022**, *12*, 14587. [[CrossRef](#)]
103. Xiong, P.; Long, C.; Zhou, H.; Battiston, R.; Zhang, X.; Shen, X. Identification of electromagnetic pre-earthquake perturbations from the DEMETER data by machine learning. *Remote Sens.* **2020**, *12*, 3643. [[CrossRef](#)]

Disclaimer/Publisher’s Note: The statements, opinions and data contained in all publications are solely those of the individual author(s) and contributor(s) and not of MDPI and/or the editor(s). MDPI and/or the editor(s) disclaim responsibility for any injury to people or property resulting from any ideas, methods, instructions or products referred to in the content.